

CHAPTER 1

INTRODUCTION

1.1. Background

The project is to study the effect of micro-size bubbles at various temperatures as method of water purification. Micro-bubbles are released from the bottom of the water column from the compressed air system. Due to buoyancy effect, these micro-bubbles will move upward and push all pollutant to the top of water column, which will then be drained away.

1.2. Problem Statement

Suspended particles can be filtered away to clean the water, which is normally a costly process. Another approach to remove the suspended particles is by injecting micro- size bubbles at the bottom of water column. These micro-bubbles would move upward due to buoyancy and help to bring the suspended particles to the top. The pollutant can, therefore, be removed using a drain system.

1.3. Objective and Scope of Study

The objective of this project is to study the effect of elevated temperature micro-bubble on different pressure and temperature. The scope of this project is to study the micro-bubbles properties at following condition

- Sintered glass with porosity of 1 μm to 20 μm
- Temperature 25°C to 90°C
- Pressure 90 kPa to 120 kPa

CHAPTER 2

LITERATURE REVIEW

For the last few decades, the behavior of air bubbles has been studied extensively by many researcher and engineers. Micro-bubbles area tiny bubbles whose diameter is less then several hundred micrometers [Akimaro Kawahara 2009]. Microbubbles have various characteristic such as excellent gas-dissolution abilities due to their very large gas-liquid interfacial area per unit volume and long stagnation, ability to be suspended uniformly, and the dynamic motion have brought great interest in industrial application as well as in fundamental studies.

In the field of medicine, micro-bubbles have many great potential applications in fields such ultrasound contrast agents, targeted drug delivery, and tumor destruction. While in food industry, the density and texture of gel and cream based foods would be controlled by the uniform and fine dispersal of gas into these materials. In the chemical industry, micro-bubbles formation is expected to be applicable in the development of porous materials such as microcellular plastic foam. [Masato Kukizaki, Tsubasa Wada (2007)]

2.1 SEPARATION PROCESS BY DISSOLVED AIR FLOATATION

Floatation is an operation used to separate solids or liquids particles from a liquid phase. The particles that will be separated is in dispersed condition, whereas the liquid phase (generally water), forms the continuous condition.

According to Bensadok, et. al. (2006), the steps that are significant and conditioning the effectiveness of the dissolved air floatation treatment are the generation of gas bubbles and the formation of the agglomerates bubbles particles.

2.2. AIR-BUBBLES FORMATION

The size of micro-bubbles in diameter is usually in the range of less than 50 micron to several hundred microns. The advantage of having smaller size bubbles is because small bubbles are more resistance to deformation. Furthermore, the shape of the bubbles, which is spherical, makes the modeling and analysis much easier to conduct. However, smaller size bubbles cannot be generated easily. This is due to limited buoyancy force which is needed to assist bubble detachment from the bubble generator (Aref, Zhenhe & Jacob, 2007). Therefore, small bubbles can only be generated if the surface tension of the liquid is sufficiently low. Aref, et. al. (2007) has suggested the use of additional surface-active agents for aqueous solution to reduce the surface tension, or additional external force to facilitate the gas bubble detachment.

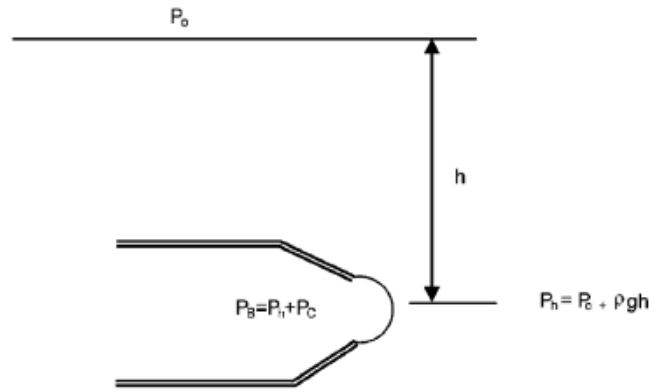


FIGURE 2.1: Pressure Distribution on a Fine Pore

For a non flow system (refer to FIGURE 1) the pressure inside the bubble (P_B) is the sum of two independent pressures, which is the hydrostatic pressure (P_H) and capillary pressure (P_C).

$$P_B = P_H + P_C$$

The capillary pressure (P_C) is the pressure difference between the inside and the outside of the bubble, which is given by Young-Laplace equation as:

$$P_C = \frac{2\gamma}{R}$$

where R is the radius of the bubble and γ is the surface tension of the liquid.

As for the hydrostatic pressure (P_H), it is the sum of atmospheric pressure (P_O) and the liquid head (h) above the system.

$$P_H = P_O + \rho gh$$

where ρ is the density of liquid, and g is the acceleration due to gravity.

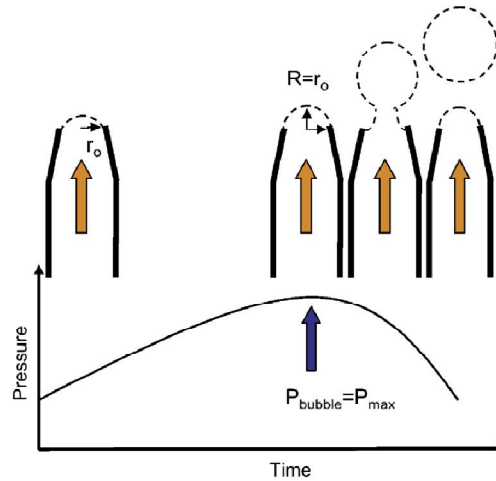


FIGURE 2.2: Bubble generation process and pressure variation time

As the compressed air flows into the fine pores at the synthetic glass, the bubble grows and the pressure inside the bubble increase. At the maximum pressure, P_{max} , the bubble it is at its smallest radius $R = r_o$ and forms a half sphere. After passing this point of maximum pressure, the pressure inside the bubble decreases spontaneously and breaks away from the fine pores at the sintered glass (see FIGURE 2).

2.3 REGION OF BUBBLES FORMATION

Bubble formation can be distinguished up to four regions (Felixtianus,2008):

1. The first region of primary bubbles where the bubbles are formed produced by the gas distributor
2. The second region of secondary bubbles is where the bubbles break-up from the diffuser.

3. The third region of dynamic equilibrium between coalescence and disruption of the bubble
4. Finally, the separation region where the bubbles reach at the top of the liquid layer

In sufficiently deep liquid layer in the water column, the third region is the subject of the present work.

2.4 BUBBLE MOTION DESCRIPTION

Air bubble can be treated as fluid, where by the motion of the air bubbles can be described by Lagrangian approach. The Lagrangian approach is basically a method of identifying one bubble and describing its motion with respect to time. The motion can be expressed in terms Cartesian coordinates as

$$\mathbf{r}(t) = x(t)\mathbf{i} + y(t)\mathbf{j} + z(t)\mathbf{k}$$

The movement of the micro-bubbles can also be describe by imagining an array of ‘windows’ in the flow field, and have the information for the velocity of the fluid particles that pass each window for all time. This approach is known as Eulerian approach.

2.5 FORCE BALANCE

For spherical bubbles, the bubble growth is described by the Rayleigh-Plesset equation (Aref, Zenghe & Jacob,2007):

$$R\ddot{R} + \frac{3}{2}(\dot{R})^2 = \frac{1}{\rho_L} \left[P_B - \frac{2\gamma}{R} - P_H \right]$$

Where R is the bubbles radius at time t , \dot{R} and \ddot{R} is the time derivative, ρ_L is the density of the liquid and P_B is the internal pressure on the bubbles.

However, during the bubble growth, three major forces balance each other and determine the size of detached bubbles. Among these force, the buoyancy force

assist the detachment, while the capillary and hydrodynamic forces resist the bubble detachment. The hydrodynamic force reduces to the added force where the drag force is neglected.

For the case where the density of the liquid is much larger than the density of the gas, we can neglect the bubble mass and write

$$\frac{d}{dt} \left(\frac{1}{2} \rho_L V_b \frac{dz}{dt} \right) + 2\pi\gamma r_0 = \rho_L V_b g$$

Where z is defined as the position of the center of bubbles with respect of the tip of the sintered glass and r_0 is the radius of the porous tip.

2.6 COLLISION AMONG BUBBLES

Another factor to be considered during the formation of the bubbles is collision. Collision is a phenomenon where the micro-bubbles is joined together to create bigger bubbles, hence resulting resistance in producing smaller bubbles in diameter.

According to study done by Revellin, et. al. (2007), bubble collision occurs when a long bubble touches a shorter bubble ahead of it and forms one longer bubble. The difference in velocities between the long and the short bubbles explains this phenomenon. The longer the vapor bubble, the faster it travels.

This experiment is based on assumption on coalescence proposed by R.Pohorecki (2005)

- The bubble coalescence rate is equal to the product of bubble collision rate and the collision efficiency.
- The bubble collisions may be caused by turbulence, buoyancy or laminar shear
- The bubble break-up rate is equal to the product of collision bubbles

2.7 DIAMETER OF BUBBLE

The resultant bubble size can be primarily determined by the pore size of the sintered glass used. However, beside pore uniformity, process parameters such as the operating pressure, flow velocity and the surface tension between the gaseous and water phases are important in generating micro-bubbles.

The average diameter of the micro-bubbles can be calculated using these equations (Felixtianus, 2006):

For distilled water

$$d = A\rho^\alpha\mu^\beta\sigma^\gamma U^\delta$$

For other liquids

$$d_{32} = 0.288\rho_L^{-0.552}\mu_L^{-0.488}\sigma^{0.442}\mu_G^{-0.124}$$

Where d is the micro-bubble diameter, ρ , μ , and σ is the fluid density, viscosity and surface tension respectfully, and U is the bubble vertical velocity

TABLE 2.1: Physiochemical properties of distilled and polluted water

Glycerin Percentage (% by volume)	Viscosity (Centipoise)	Density (g/cm ³)	Surface Tension (mN/m)
0.0 (Distilled Water)	1.0	1.0000	73
0.1	1.5	0.9975	53
0.2	1.2	0.9979	55
0.3	1.2	0.9983	59
0.4	1.2	0.9986	63
0.5	1.1	0.990	67
Residential Waste Water	1.2	0.9882	55

2.8 MEASUREMENT OF BUBBLES DIAMETER

Various methods have been used to assess micro-bubble size, such as X-Ray attenuation, laser based techniques, empirical or semi empirical correlation based on fluid dynamics, electro resistivity measurements and image analysis. Image analysis is reported as the most widely method used, however it has some disadvantages, such as requiring transparent wall for the image acquisition, low bubble concentration and complicated experimental set-up. It also time consuming despite modern high-speed CCD Camera.

Laser Doppler Anemometry (LDA) is a technology used to measure velocities of flows or more specifically of small particles in flows. The technique is based on the measurement of laser light scattered by particles that pass through a series of interference fringes (a pattern of light and dark surface). The scattered laser light oscillates with a specific frequency that is related to the velocity of the particles. If the flow is perpendicular to the fringes the relation between this frequency f_d , and the velocity v_x is determined by the angle 2θ between intersecting laser beams and the wavelength of the laser beam

$$f_d = 2 \sin \theta \frac{v_x}{\lambda_0}$$

2.9 FLOATATION OF FINE PARTICLES

Floatation is a separation treatment process that uses small bubbles to remove low density particulates from potable water and wastewaters. Small air bubbles are generated at the bottom of the water to be treated. The bubbles rise to the surface of the liquid, acting as collectors of fine particles in the solution. Floatation is also known as electro-floatation, dissolved air floatation and dispersed air floatation, depending on the methods that being use to generate the bubbles in the system. [S.E Burn et al. 1997]

The poor recovery of fines by floatation can be contributed to the low probability of bubble –particle collision, which decrease with the decreasing particle size. However, bubble-particle interactions such as electrostatic and hydrophobic force are important in determining the selectivity of a separation. In conventional froth floatation, particle and bubbles that are oppositely charged are attracted; however, the particles must also be sufficiently hydrophobic to rupture the wetting films between the particles and bubbles in order to the bubbles. [K.E Water et al. 2007]

Furthermore, froth phase mechanism such as entrainment plays an important role in the recovery of particles to the concentrate. Fine particles have a higher tendency to be entrained into the froth in the channels between bubbles or in the turbulent region surrounding a bubble or in the turbulent region surrounding a bubble due to their lower mass and momentum. Entrainment is non selective, therefore while increasing the recovery of particles to the concentrate, it also tends to lower the grade of concentrate [K.E Water et al. 2007]

While the probability of collision decreases with decreasing particle size, it is inversely proportional to bubble size, suggesting that improved fine particles recovery can be obtained by floatation using small bubbles. This has been the focus of many studies, with such methods of generation of small bubbles including dissolved air floatation and pico bubbles. [K.E Water et al. 2007]

2.10 **DISPERSED AIR FLOATATION TECHNIQUE**

Dispersed air floatation technique is another way of generating micro bubbles through the use of a bubble diffuser. In this method, the micro bubble is produced at the bottom of the column and the compressed air is forced through the pores of fixed size to produce the micro bubbles. This method of treatment has been used to remove particulate materials, such as quartz particles, with diameter less than 50 μm . [S.E Burn et al. 1997]

Some research done by Ahmed and Jameson, by forcing pressurized gas through a sintered glass disc with fixed pore size, produced micro bubbles with diameters from 75 to 655 μm , showing that smaller diameters yielded higher particulate removal rates. Another study done by Huang et al. has used this method to generate bubbles for the removal of heavy metals from solution by adding a coagulant to initiate the flocculation of particles present in the solution. [S.E Burn et al. 1997]

CHAPTER 3

METHODOLOGY

In order to achieve the objective of the project, experimental lab work and number of trials has to be performed in order to observe the behavior of the elevated micro-bubbles. Hence, appropriate apparatus has to be identified and set up before the experiment being done. In the present experiments, an approach by Felixtianus is used.

For experimental purpose, a test rig of a water column of 100mm length, 100mm width, and 240 mm height was set up. A diffuser was mounted at the bottom of the water column. Various porosities of sintered glass were used to produce air bubbles. Pressurized air is pump through the diffuser. Glycerin solution was used to manipulate the variations of surface tension, density and viscosity.

The water column was equipped with flow meter, thermometer and monometer to measure the input air conditions. Air was inducted into the water column using compressor and controlled by a pressure regulator. Before reaching the diffuser holes, air pressure, air flow rate and temperature was measure. The experiments were conducted at ambient pressure and room temperature conditions. The gas phase was air for all runs, with tap water. The height of the liquid is 200mm. The process flow chart is as below:

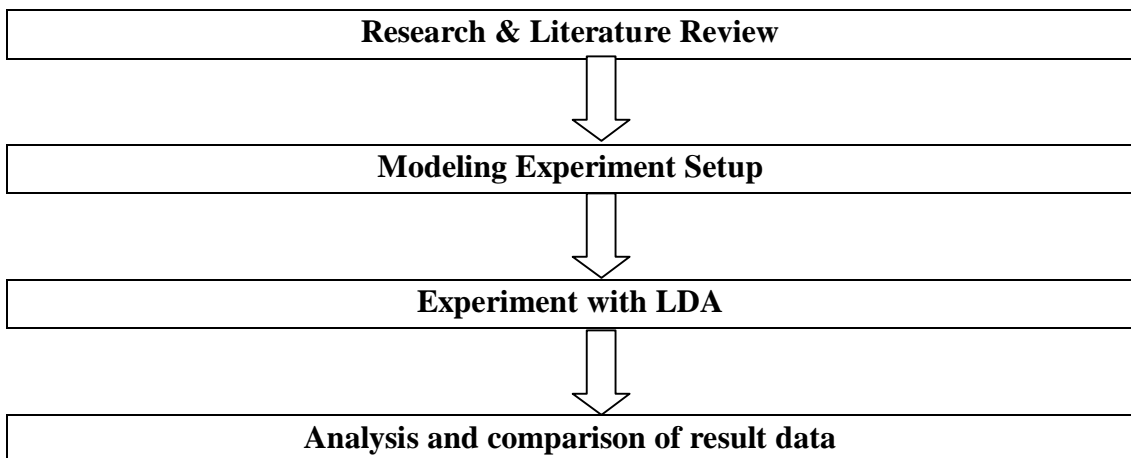


Figure 3.1: Process Flow Chart

3.1 EXPERIMENT SETUP

The experiment set-up consists of small vertical water column with a square cross-section of side length of 100mm and height 240mm. A two 5 meter long plastic tubes installed at the centre of the bottom plate are used for the air injection. The experiment setup is as shown in figure

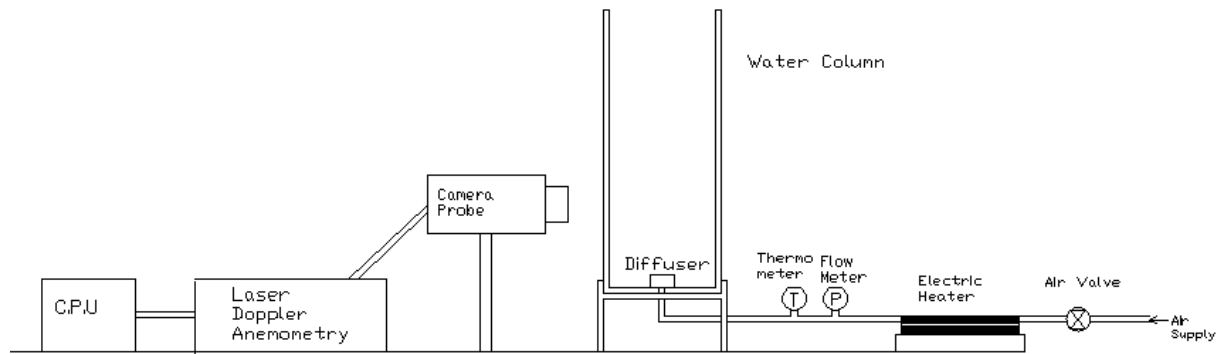


FIGURE 3.2: Schematic Diagram of Testing System

3.2 AIR SUPPLY

The air is supplied by the air compressor.



FIGURE 3.3: Air Compressor

The compressor specification is as follows:

Maximum Pressure : 115 PSI

Maximum Air Delivery : 6.3 CFM

3.3 PLASTIC TUBE

A plastic tube of 5 meter long is installed at the center of the bottom plate used for the gas injection. A plastic tube is selected due to its low thermal conductivity property compare to a metal pipe. Therefore, heat loss due to conduction and convection through the piping can be minimized.



FIGURE 3.4: Pipe Hose to Supply Air

3.4 FLOW METER, THERMOMETER AND MONOMETER

In this project, the piping is equipped with flow meter, thermometer and monometer to measure the input air conditions. Air was pump into the water column using the air compressor and controlled by a pressure regulator. The flow is set to be constant in order to understand the effect of the temperature to the dynamic behavior of the micro-bubbles. The flow rate inside the tube is controlled by verifying the valve.



FIGURE 3.5: Flow Meter and Thermometer before entering the water column

3.5 HEATING MECHANISM

The heating mechanism used is by using a copper tube which is heated by burning the LPG Gas on gas stove. The piping system from the air supply is then connected to the copper tube and heated. Another end of the copper tube is connected to the water column.



Figure 3.6: The copper tube on the stove



Figure 3.7: Inside view of the copper tube

3.6 SINTERED GLASS WITH FINE PORES

The synthetic glass with fine pores acts like a diffuser. It is mounted on the bottom of the water column to produce micro-size bubbles by passing the air through it before reaching the water. The bubbles would emerge from the surface of sintered glass. In this experiment, the synthetic glass with porosity of 1 – 10 micron is selected to produce the micro-size bubbles.

Bubble growth on the sintered glass takes place under constant flow rate. In addition the pressure of air pump into the system is also constant, since the volume is very large compared to the diameter of the tube.

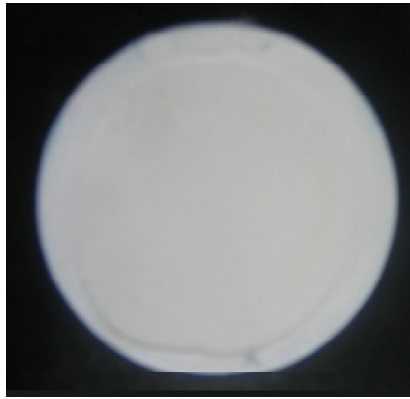


FIGURE 3.8: Sintered Glass with Porosity of 1 to 10 micro in diameter

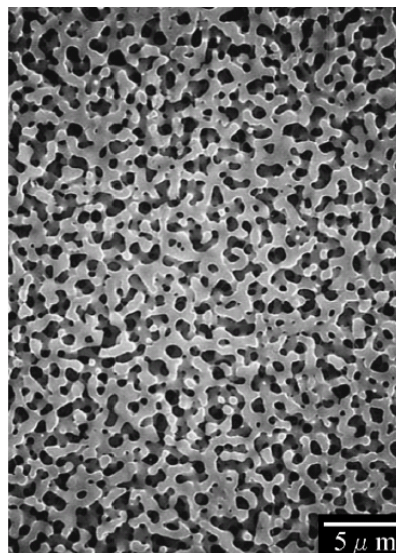


FIGURE 3.9: SEM image of sintered glass with porosity of 5micro meter in diameter

3.7 TEST RIG - WATER COLUMN

The water column is made transparent so then the pattern can be seen. There are two types of water column, which are cylindrical and rectangular. In this project, a 100 mm x 100 mm x 240 mm rectangular water columns has been selected for the experimental purpose.

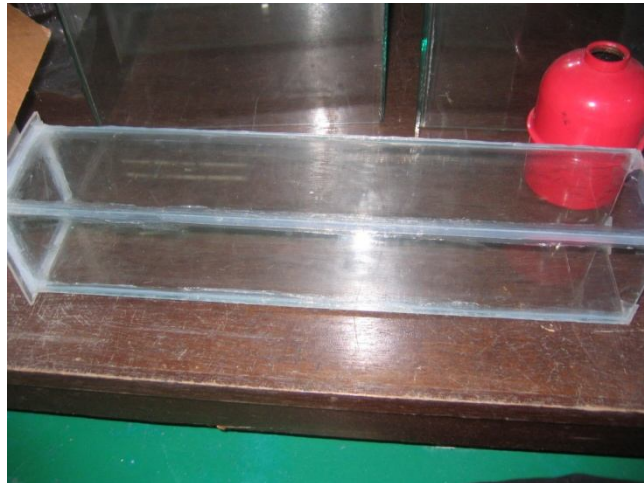


FIGURE 3.10: Water Column



FIGURE 3.11: Water Column attached to the sintered glass

3.8 LDA EQUIPMENT

Laser Doppler Anemometry (LDA) equipment is used to measure the direction and speed of the fluid particle. In this project, LDA is used to measure the vertical and horizontal velocities of the bubbles as well as the micro-bubbles diameter. LDA is employed to aim insight into the phenomena occurring during the bubble formation on the water column. The camera probe is fixed on the stand very close to the area of observation.

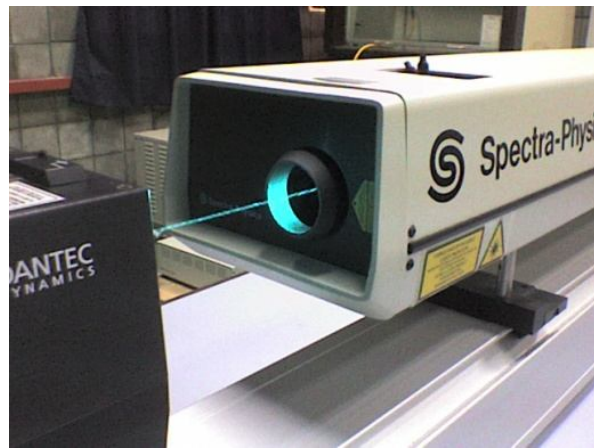


FIGURE 3.12: Laser Doppler Anemometry (LDA) machines



FIGURE 3.13: LDA Camera Probe

3.9 GANTT CHART

The research and project work have been done according to the following schedule:

No	TASK	SEMESTER I July 2008						SEMESTER II July 2009					
		JULY	AUG.	SEPT.	OCT.	NOV.	DEC.	JULY	AUG.	SEPT.	OCT.	NOV.	DEC.
1	Selection Of Project Topic	■											
2	Preliminary Research Work		■										
3	Submission of Preliminary Report		■										
4	Literature Review & Research Work		■	■	■								
5	Submission of Progress Report				■								
6	Seminar					■							
7	Submission of Interim Report						■						
8	Oral Presentation						■						
9	Project Continue						■	■					
10	Submission of Progress Report I							■					
11	Project Continue							■	■				
12	Submission of Progress Report 2								■	■			
13	Seminar									■			
14	Poster Exhibition									■			
15	Submission of Dissertation Final Draft										■		
16	Oral presentation											■	
17	Submission of Project Dissertation												■

FIGURE 3.13: Gantt chart for the overall Final Year Project (Semester I and II)

CHAPTER 4

RESULT & DISCUSSION

4.1 Result

a) Micro-bubble properties with Sintered Glass G-1 (Porosity of $1\mu - 10\mu$)

Table 4.1: Summary of Micro-bubbles properties at flow rate ($\dot{V}=5$ liter/min)

Time (min)	Air Inlet Pressure (kPa)	Temperature ($^{\circ}\text{C}$)			Average Diameter (μm)	Average Velocity (m/s)	
		Ambient Air	Heated Air	Water		Vertical	Horizontal
0	112	25	92.6	26.1	22	0.2	0.4
15	112	25	93.8	26.1	42	0.1	0.7
30	112	25	95.8	26.1	68	0.1	0.5
45	112	25	96.8	26.1	91	0.2	0.4
60	112	25	98.6	26.1	140	0.1	0.6
75	112	25	100.4	26.2	144	0.1	0.6

b) With Sintered Glass with Sintered Glass G-2 (Porosity of $10\mu - 20\mu$)

Table 4.2: Summary of Micro-bubbles properties at flow rate ($\dot{V}=5$ liter/min)

Time (min)	Air Inlet Pressure (kPa)	Temperature ($^{\circ}\text{C}$)			Average Diameter (μm)	Average Velocity (m/s)	
		Ambient Air	Heated Air	Water		Vertical	Horizontal
0	92	24	55.3	25	16	0.1	0.4
15	100	24	82.9	25	52	0.1	0.4
30	110	24	88.4	25	56	0.1	0.4
45	110	24	99.7	25	120	0.1	0.7
60	110	24	104.9	25	112	0.2	0.5
75	110	24	105.4	25	148	0.2	1.2

4.2 Discussion

4.2.1 Effect of air inlet pressure on micro-bubble diameter

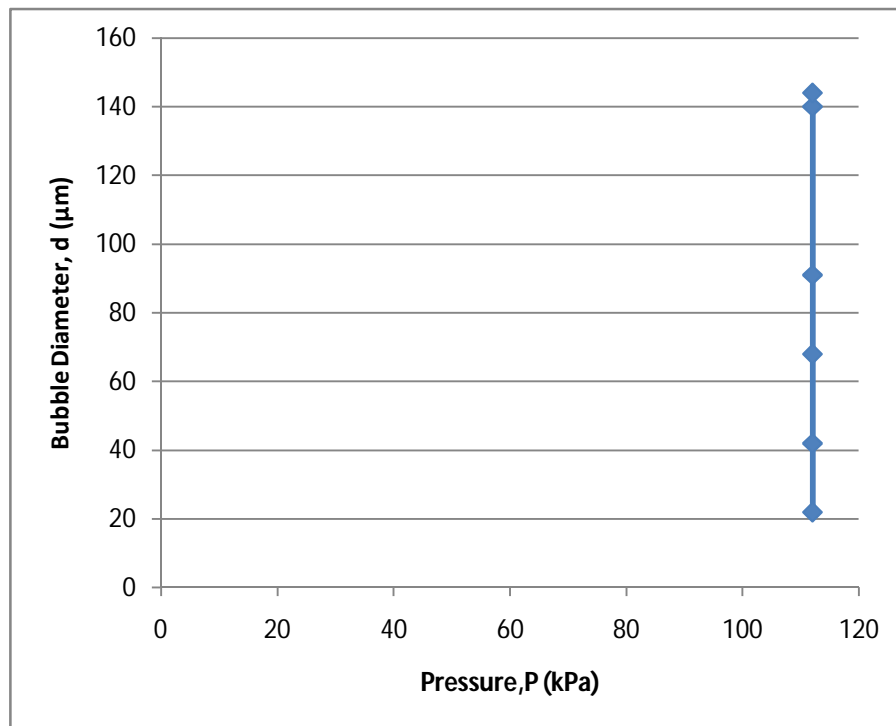


Figure 4.1: Bubble Diameter Vs Air Inlet Pressure for Sintered Glass SG-1 ($1\mu - 10\mu$)

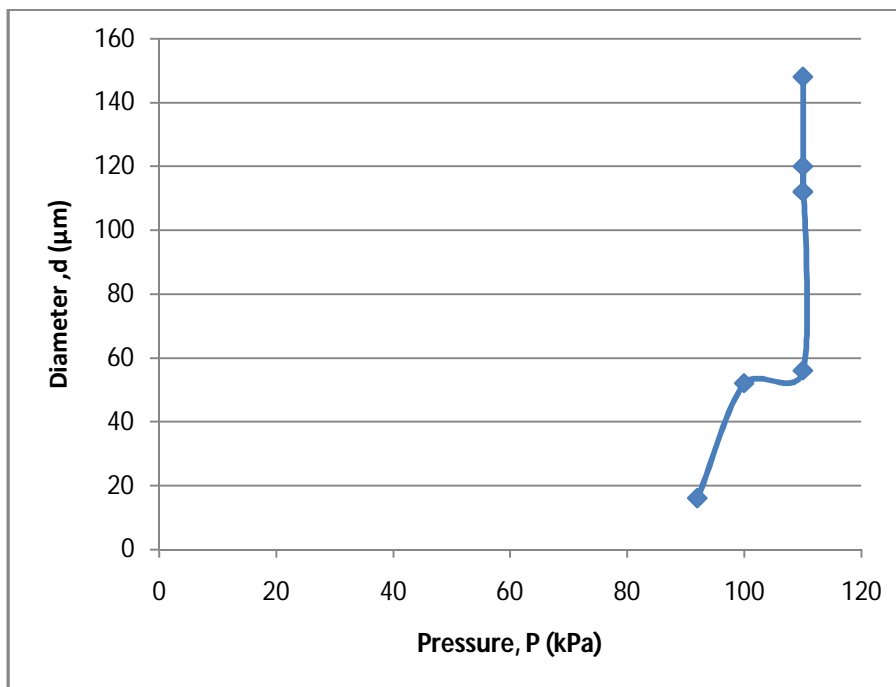


Figure 4.2: Bubble Diameter Vs Air Inlet Pressure for Sintered Glass SG-2 ($10\mu - 20\mu$)

As we can see from the graph, it shows that, by the air inlet pressure increase, the bubble diameter is also increase. However, at a constant pressure, the diameter of the bubbles can be further increase by increasing the temperature of inlet air to the system (See Section 4.2.2).

We can also observe that by the time the injection bubble pressure reach constant (110 kPa), the diameter of the bubble for of sintered glass G-2 is bigger than sintered Glass G-1. This is because sintered glass G-2 has higher porosity compared to sintered Glass G-1.

4.2.2 Effect of temperature on micro-bubble diameter

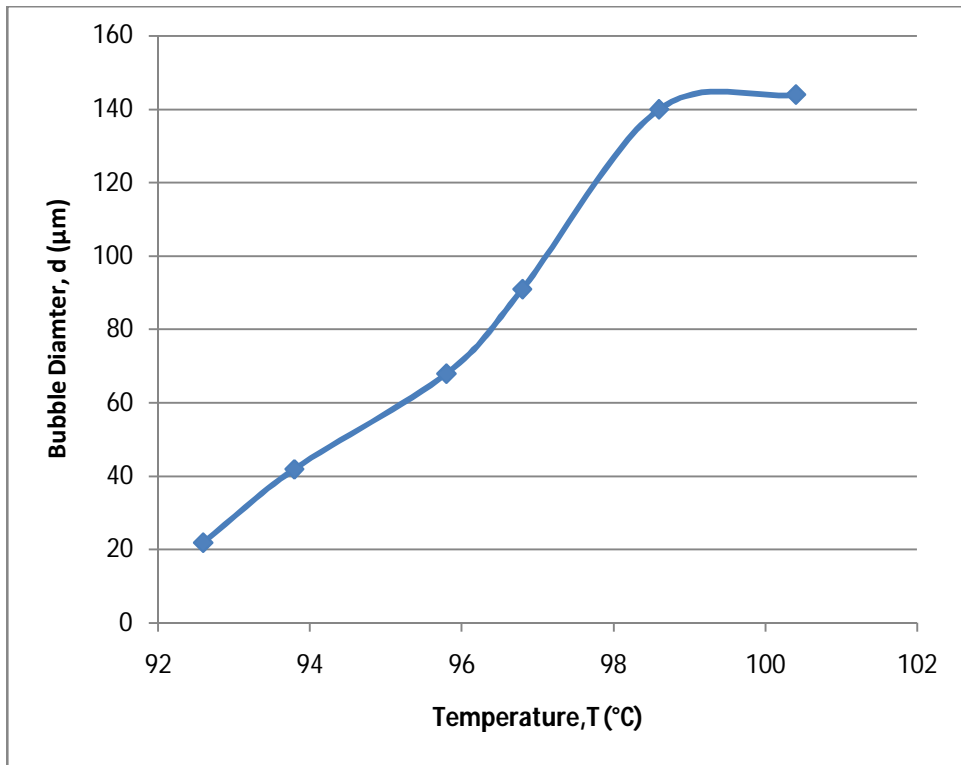


Figure 4.3: Bubble Diameter Vs Temperature for Sintered Glass (1µ – 10µ)

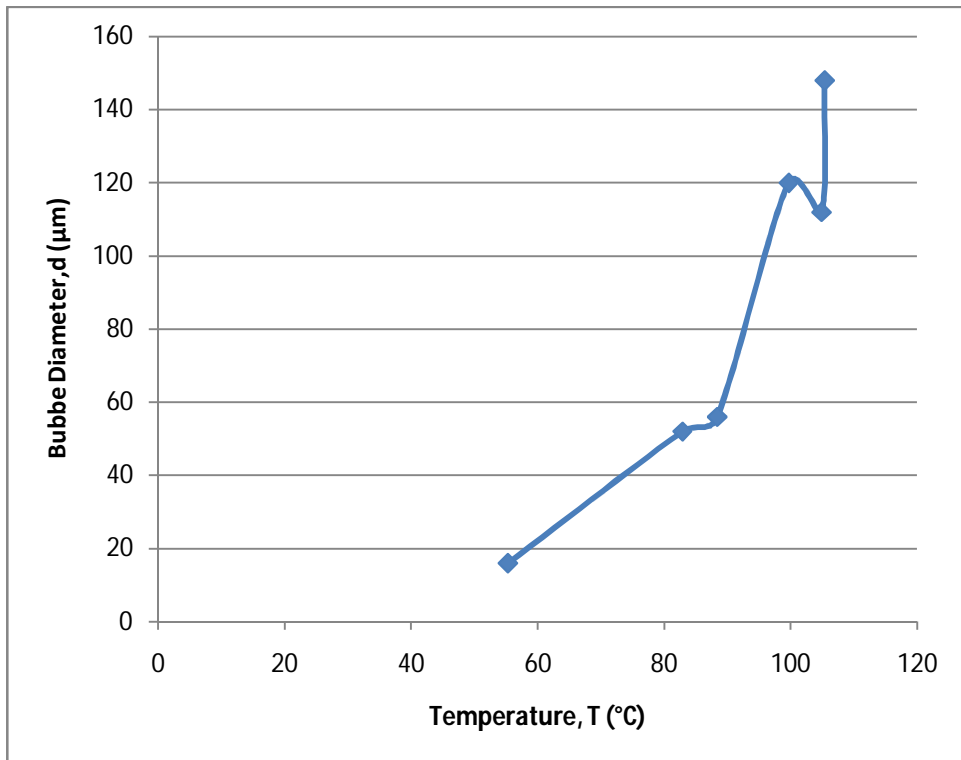


Figure 4.4: Bubble Diameter Vs Temperature for Sintered Glass (10µ - 20µ)

As we can see from the graph, it shows that, as the inlet air temperature is increased, the bubble diameter is also increasing. Even though the air inlet pressure is at constant, the diameter of the bubbles can be further increase by increasing the temperature of inlet air to the system.

We can also observed the sintered glass G-2 required lower temperature to compare sintered glass G-1 to reach bigger diameter bubbles. This is because sintered glass G-2 has higher porosity compared to sintered Glass G-1.

The relationship of bubble diameter and air inlet temperature can be estimated through the following formula

4.2.3 Effect of Air Inlet Pressure on Bubble Velocity

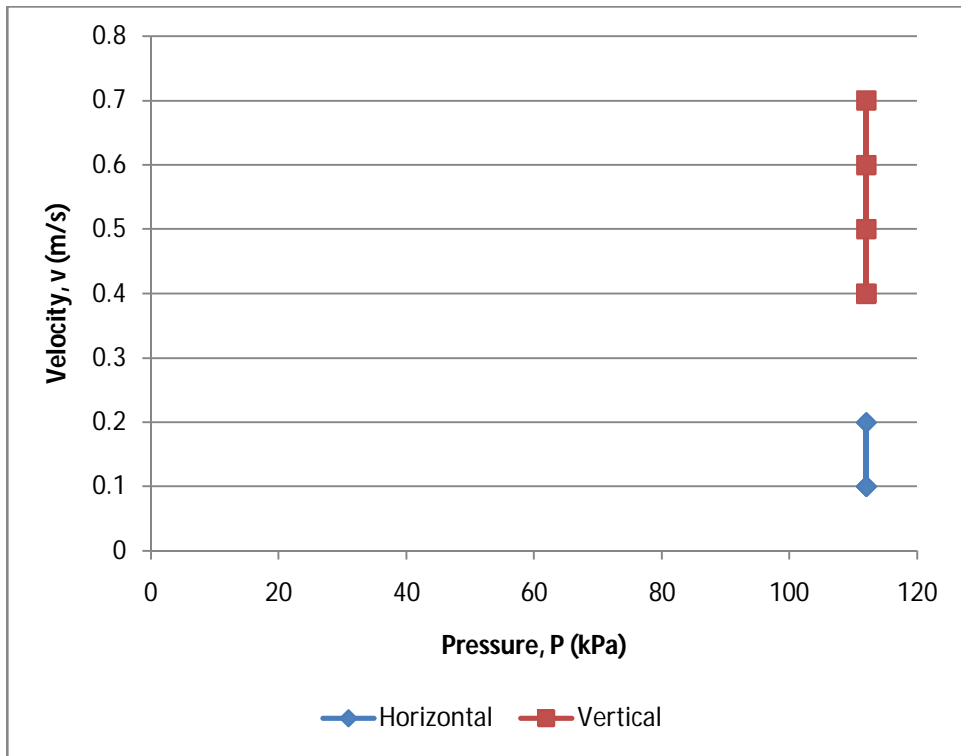


Figure 4.5: Bubble Velocity Vs Air Inlet Pressure for Sintered Glass ($1\mu - 10\mu$)

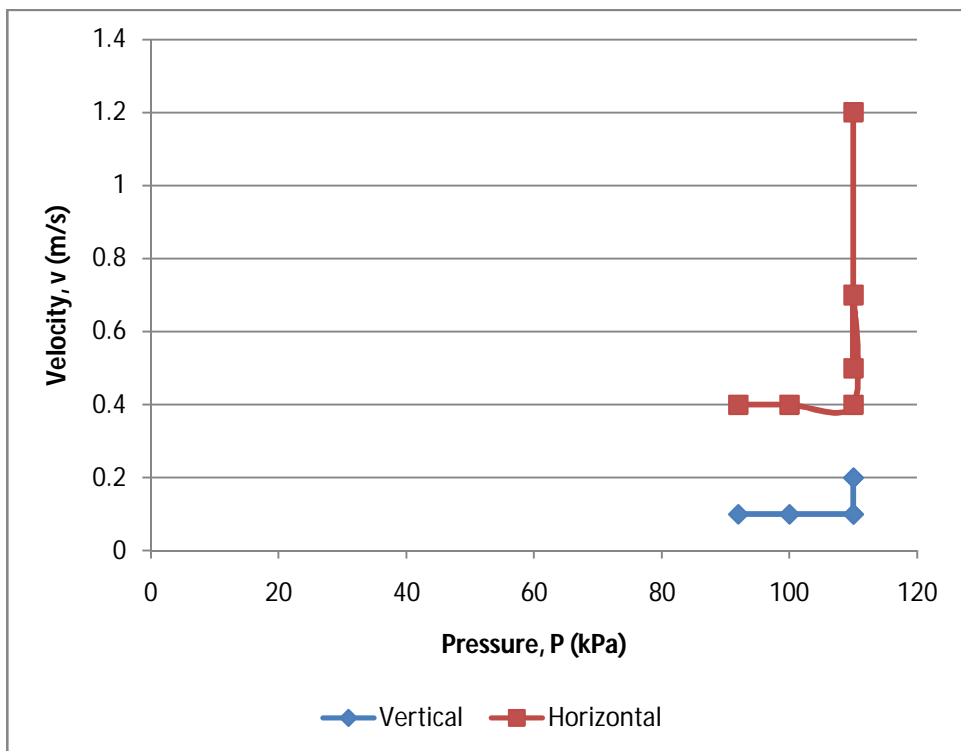


Figure 4.6: Bubble Velocity Vs Air Inlet Pressure for Sintered Glass ($10\mu - 20\mu$)

As we can see from the graph, it shows that, as the inlet air inlet pressure increased, the bubble horizontal velocity is increased and vertical velocity is decrease. Even though the air inlet pressure is at constant, the diameter of the bubbles can be further increase by increasing the temperature of inlet air to the system.

For sintered glass SG-2 (with porosity of $10\mu - 20\mu$), the relationship between bubble velocity and air inlet pressure can be estimated using equation

4.2.4 Effect of Air Inlet Temperature on Velocity of Micro-bubbles

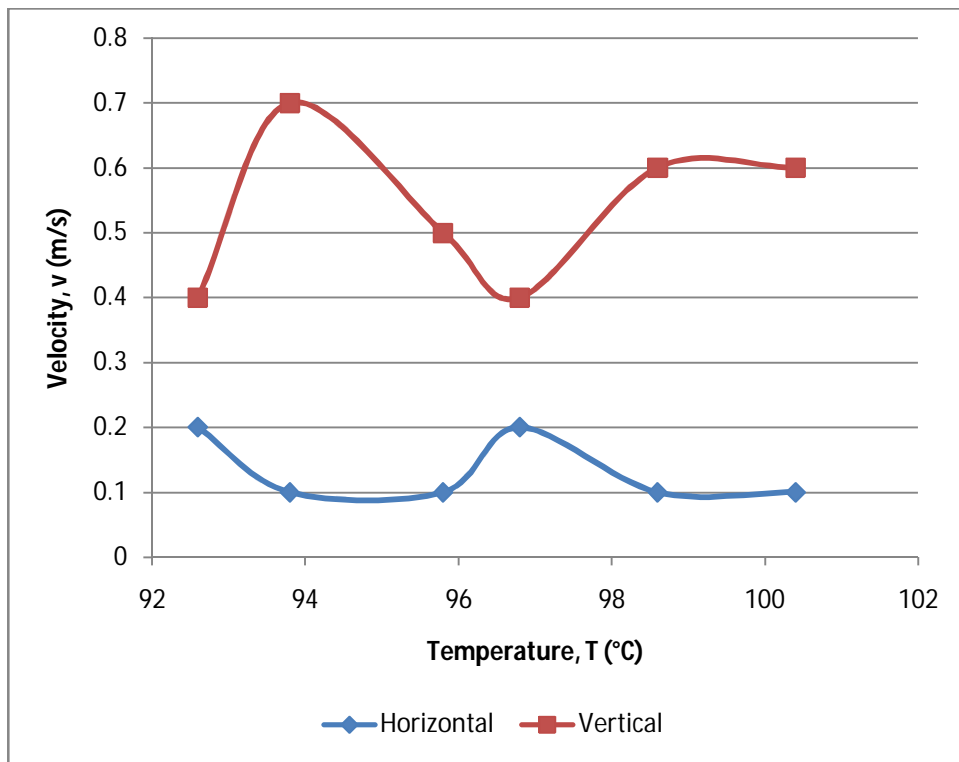


Figure 4.7: Bubble Velocity Vs Air Inlet Temperature for Sintered Glass (1μ -10μ)

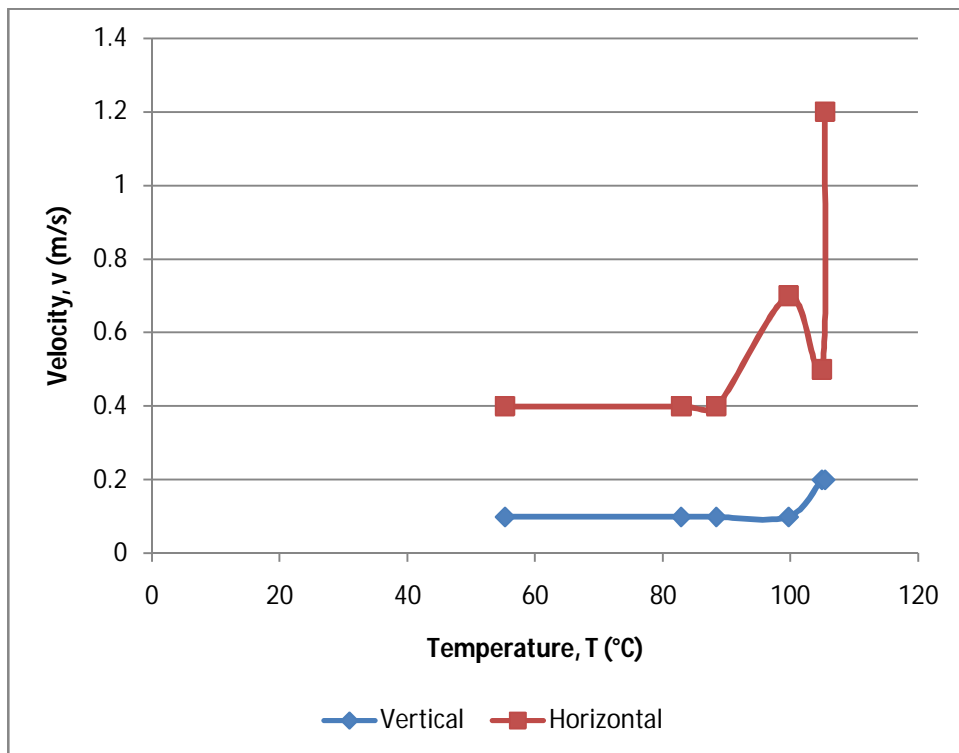


Figure 4.8: Bubble Velocity Vs Air Inlet Temperature for Sintered Glass (10μ -20μ)

As we can see from the graph, it shows that, by increasing the inlet temperature of air, the bubble velocity in vertical direction is horizontal direction is decreasing while the bubble velocity in horizontal direction is increasing.

This is because, when the temperature and pressure increase, the bubble gained more energy, hence moving horizontally with increasing speed. However, as the temperature and pressure increase, the micro-bubble size is also increasing, which make the bubble more heavy yet moving in vertical direction. As we increase the pressure and temperature, we will expect zero vertical velocity but with bigger bubble diameter in size.

We can also observed the sintered glass G-2 required lower temperature compare sintered glass G-1 to reach bigger diameter of the micro bubbles. This is because sintered glass G-2 has higher porosity size compared to sintered Glass G-1.

4.2.5 Effect of Bubble Diameter on Bubble Velocity

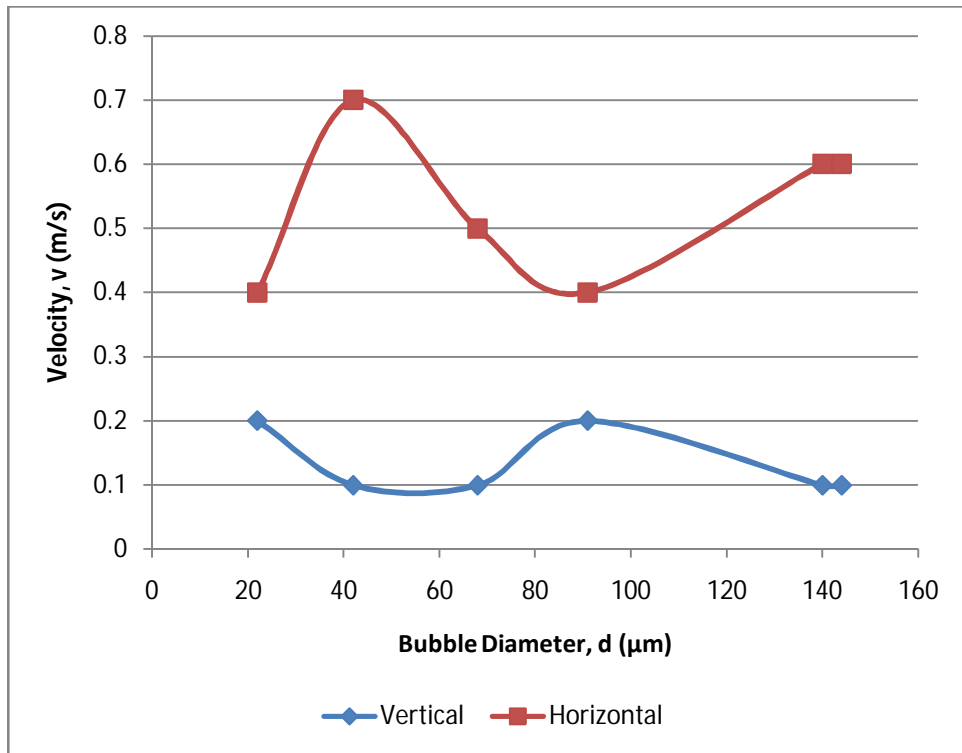


Figure 4.9: Bubble Velocity Vs Bubble Diameter for Sintered Glass (1μ - 10μ)

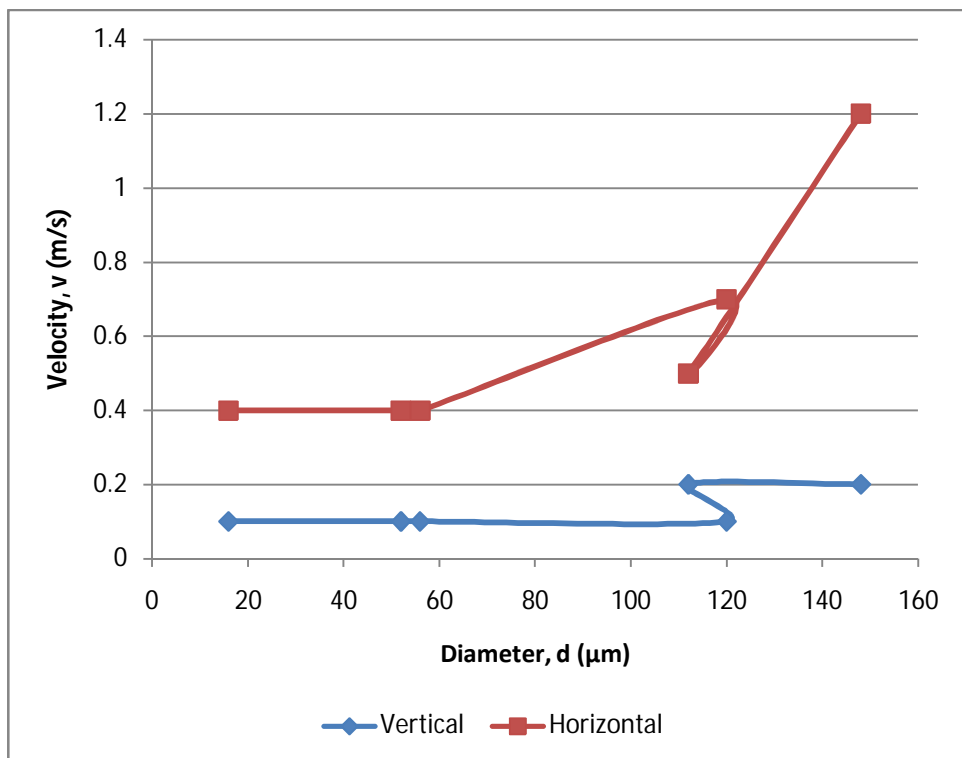


Figure 4.10: Bubble Velocity Vs Bubble Diameter for Sintered Glass (10μ - 20μ)

As we can see from the graph, it shows that, by increasing the diameter of the bubble, the bubble velocity in vertical direction is horizontal direction is decreasing while the bubble velocity in horizontal direction is increasing.

This is because, when the temperature and pressure increase, the bubble gained more energy, hence moving horizontally with increasing speed. However, as the temperature and pressure increase, the micro-bubble size is also increasing, which make the bubble more heavy yet moving in vertical direction..

CHAPTER 5

CONCLUSION & RECOMMENDATION

5.1 Conclusion

The study of single micro bubble in a liquid helps in order to understand in the fundamental studies and industrial application, such as bubble rise velocity, bubble-bubble collision, bubble-particle interaction and bubble solid attachment.

Application of Laser Doppler Anemometry (LDA) technique to analyze bubbles produced in the process allowed for determination of equivalent bubble diameter produced, bubbles raise velocity and horizontal bubble velocity.

As the pressure increase, the bubble diameter also increase. This is because the detachment of the bubble is depended on the pressure. Even though the pressure is constant, the micro-bubble diameter can be increase by increasing the air inlet temperature, which also increasing the pressure (Ideal Gas Law).

As the pressure and temperature increase, the velocity of the bubble in horizontal direction is increasing while the velocity in vertical direction is decreasing. This is because, as the pressure and temperature increase, there is also increasing in size, which make the bubble gain weight, hence its will moving to the vertical direction to compensate the acting force. However, as pressure and temperature increase, the vertical velocity will moving toward zero velocity (no movement in vertical direction). However, this will also increase the diameter of the bubbles.

Zero horizontal velocity is required in order to achieve linear rise up movement of micro bubble. The liquid is also need to be stable, which turbulence effect is at minimum. As the pressure increase, the horizontal velocity is increase, however, is neglected because the reading is small. As the pressure increase, it is observed that the diameter of the micro-bubbles is also increased.

5.2 Recommendation

Single bubbles are more resistant to deformation and their spherical shape makes their analysis and modeling of bubble-related phenomenon much easier to conduct. A single micro bubble can be produce using micro-pipette, where the micro-bubble size is depend on the micropipette tip size, taper length, inclination angle and gas type.

Little attention has been paid to the influence of the surface wettability in the study of relatively large bubble formation from a nozzle, orifice or porous plate. This is because the surface wettability had a negligible effect on the large bubble formation.

To obtain better results, an air leakage from the sintered glass holder to the test rig (water column) should be avoided. This will produce bigger bubble in diameter which will mix with the smaller bubble in the system. This is not desirable since it will affect the reading taken the Laser Doppler Anemometry (LDA) equipment.

Another way to obtain better result is to change current test rig (water column) with lower diffraction index glass. The measurement are performed at the intersection of two laser beam, where there is an interference fringe pattern of alternating light and dark planes. By having lower diffraction index, the laser beam will intersect better, hence

REFERENCES

1. Crowe, Elger & Roberson (2005) *Engineering Fluid Mechanics 8 Edition*, John Wiley & Sons, Inc United State
2. Aref S.N, Zhenghe X. & Jacob M. (2007): *Single Micro-bubble Generation by Pressure Pulse Technique*, Chemical Engineering Science 63 Elsevier Limited
3. Revellin R., Agostini B., & Thome J. R. (2007): *Elongated Bubbles in Microchannel. Part II: Experimental Study and Modelling of Bubble Collisions*, Multiphase Flow 34, Elsevier Limited
4. Bensadok K., Belkacem M., & Nezzal G. (2006): *Treatment of Cutting Oil/Water Emulsion by Coupling Coagulation and Dissolved Air Floatation*, Desalination 206, Elsevier Limited.
5. Felixtianus Eko Wismo Winarto (2008): *Effect of Impurities On The Dynamic Behavior of Micron Air Bubbles In A Water Column*, UTP 7th Biannual Postgraduate Research Symposium (2008)
6. Akimaro K., Michio S., Fuminori M., Hidetoshi M., Mayo.T, Masanori N. (2009) *Prediction of Micro-Bubble Dissolution Characteristic In Water and Sea Water*, Experimental Thermal and Fluid Science, ScienceDirect
7. R. Pohorecki, W. Maniuk, P.Bielski, P.Sobieszuk, G.Dabrowiecki (2005) *Bubble diameter correlation via numerical experiment* Chemical Engineering Journal 113, Elsevier
8. M.Kukizaki, T. Wada (2007) *Effect of membrane wettability on the size and size distribution of microbubbles from Shirasu-porous-glass (SPG) membrane*, Colloids and Surfaces A: Physicochem. Eng Aspect 317, Elsevier
9. N.A Kazakis, A.A.Mouza, S.V. Paras (2008), *Coalescence during bubble formation at two neighbouring pores: An experimental study in microscopic scale*, Chemical Engineering Science 63 Elsevier
10. S.E Burns, S. Yiacomi, C.Touris (2007) *Microbubbles generation for environmental and industrial separation*, Separation and Purification Technology 11 221-232 Elsevier
11. John R Thome, Vincent Dupont (2005): *Bubble Generator. Patent No US 2005/027941 A1* United State

12. Tadao Matsumo (2007): Method of generating micro gas bubble in liquid and gas bubble generation apparatus. *Patent No US 2007/0152357 A1* United State
13. Jeremy Wickins (2001): Waste Water Treatment Apparatus *Patent No US 6210580 B1* United State
14. Yamasaki, Keichiro & Kazumi (2006) : Water treatment method and water treatment apparatus *Patent No EP 1767496 A1* Europe
15. Ken Yap, *Micro-Bubbles and Its Application* from Suwa Precision Group Website <http://www.suwaprecision.com/SIV/microbubblesapplications.html>